Accurate density functionals: Approaches using the adiabatic-connection fluctuation-dissipation theorem

Martin Fuchs and Xavier Gonze

Unité PCPM, Université Catholique de Louvain, 1348 Louvain-la-Neuve, Belgium

Fully nonlocal exchange-correlation functionals derived from the adiabatic-connection fluctuation-dissipation theorem can go beyond local or gradient corrected functionals and include the van der Waals interaction. We implement three functionals of this class, in a pseudopotential plane-wave framework, (1) using the random-phase approximation (RPA), (2) adding to the RPA short-range correlations (RPA+), and (3) including density fluctuations through an exchange kernel. We find the binding energy of the H_2 and Be_2 molecules described, by all three functionals, within 0.1 eV accuracy.

Kohn-Sham density-functional theory[1,2] is an important method for electronic structure calculations of complex (bio-) molecular and solid-state systems. In this theory, the electronic energy $E[n]$ is established as a functional of the electron density n, and includes the exchange-correlation (XC) energy $E_{XC}[n]$ to account for many-electron interactions. Practical calculations always use approximations for the XC energy (whose exact functional form is not known, at variance with all other components of $E[n]$). The usual local-density (LDA) (Ref. 2) and generalized gradient approximations (GGA's) (Ref. 3) often yield a realistic account of solids, surfaces, and molecules, in particular of their equilibrium atomic structure. Regarding molecular interactions and the related potential energy surfaces, GGA's have marked a major advance over the LDA, but yet more accurate functionals are needed to resolve critical shortcomings: GGA's (1) still fail to predict molecular dissociation energies and heats of reaction with chemical accuracy (to within 50 meV), (2) tend to underestimate activation energy barriers, and, like the LDA, (3) do not properly describe van der Waals interactions between distant subsystems.

Progress can be achieved by explicitly considering the truly nonlocal nature of both exchange and correlation, which (semi-) local approximations such as the LDA or GGA cannot account for. Hybrid functionals[4,5] that combine the exact nonlocal (Fock) exchange with local-density functionals usually perform more accurately than pure GGA's,[6] though not systematically within chemical accuracy and with limitations for molecular transition states. van der Waals forces, on the other hand, are due to long-range correlations; as such they are beyond the scope of the LDA, GGA's, or hybrid schemes and rather require a fully nonlocal correlation functional.

In this study we demonstrate that accurate, fully nonlocal exchange-correlation functionals can be implemented as approximations to the exact adiabatic-connection fluctuation-dissipation theorem (ACFDT) (Ref. 7) for the exchange-correlation energy of an electronic system,

$$E_{XC}[n] = -\frac{1}{2}\int_0^1 d\lambda \int d^3r\, d^3r' \frac{e^2}{|\mathbf{r}-\mathbf{r}'|}$$
$$\times \left[\frac{\hbar}{\pi}\int_0^\infty du\, \chi_\lambda(\mathbf{r},\mathbf{r}';iu) + n(\mathbf{r})\delta(\mathbf{r}-\mathbf{r}')\right]. \quad (1)$$

Here $\chi_\lambda(\mathbf{r},\mathbf{r}';iu)$ is the imaginary-frequency density response function of the system with the electrons interacting by a scaled Coulomb potential $\lambda e^2/|\mathbf{r}-\mathbf{r}'|$ and moving in a modified external potential such that the density stays the same as for the physical ($\lambda=1$) ground state. For $\lambda=0$, one deals with the noninteracting Kohn-Sham system; its response function is given explicitly by the Kohn-Sham eigenstates $\phi_{k\sigma}(\mathbf{r})$ and eigenvalues $\varepsilon_{k\sigma}$ as

$$\chi_0(\mathbf{r},\mathbf{r}';iu) = \sum_{\sigma,k,l} \frac{(\gamma_{k\sigma}-\gamma_{l\sigma})}{i\hbar u - (\varepsilon_{l\sigma}-\varepsilon_{k\sigma})}$$
$$\times \phi_{k\sigma}^*(\mathbf{r})\phi_{l\sigma}(\mathbf{r})\phi_{l\sigma}^*(\mathbf{r}')\phi_{k\sigma}(\mathbf{r}'), \quad (2)$$

where the sum includes all occupied ($\gamma_{k\sigma}=1$) and unoccupied ($\gamma_{k\sigma}=0$) states. For $\lambda>0$, the interacting and the Kohn-Sham response functions are related by a Dyson-type screening equation

$$\chi_\lambda(\mathbf{r},\mathbf{r}';iu) = \chi_0(\mathbf{r},\mathbf{r}';iu) + \int d^3r_1 d^3r_2 \chi_0(\mathbf{r},\mathbf{r}_1;iu)$$
$$\times f_\lambda^{HXC}(\mathbf{r}_1,\mathbf{r}_2;iu)\chi_\lambda(\mathbf{r}_2,\mathbf{r}';iu), \quad (3)$$

with the Coulomb and exchange-correlation kernel $f_\lambda^{HXC}(\mathbf{r},\mathbf{r}';iu) = \lambda e^2/|\mathbf{r}-\mathbf{r}'| + f_\lambda^{XC}(\mathbf{r},\mathbf{r}';iu)$ established in the context of time-dependent density-functional theory.[8] The set of Eqs. (1)–(3) may be refered to as ACFDT formalism and formally yields the exact density-functional exchange-correlation energy.

The correlation part of E_{XC} and the exchange part can be separated as shown in Ref. 9: The exchange energy E_X is equal to the expansion Eq. (1) with χ_λ set to χ_0, or, equivalently, to the well-known expression

$$E_X[n] = -\frac{e^2}{2}\sum_\sigma \int d^3r\, d^3r' \frac{\left|\sum_k^{occ} \phi_{k\sigma}^*(\mathbf{r})\phi_{k\sigma}(\mathbf{r}')\right|^2}{|\mathbf{r}-\mathbf{r}'|},$$
$$(4)$$

and the correlation energy is defined as $E_C[n] = E_{XC}[n] - E_X[n]$. For practical purposes one needs to use an approximation for the frequency-dependent, spatially nonlocal kernel $f_\lambda^{XC}(\mathbf{r},\mathbf{r}';iu)$ whose explicit form is unknown.

We consider three different functionals, built on two approximate XC kernels. The first kernel, within the random-phase approximation (RPA), amounts to neglecting exchange and correlation effects in f_λ^{HXC} altogether, setting $f_\lambda^{XC-RPA} = 0$. The RPA still treats E_X exactly and includes van der Waals interactions,[9] but misses important contributions from short-range correlations.[10] Following Ref. 10 we therefore also combine the RPA with a local-density correction for short-range correlations $E_C^{sr}[n] = E_C^{LDA}[n] - E_C^{LDA-RPA}[n]$, where $E_C^{LDA-RPA}[n]$ is the local-density approximation based on the RPA correlation energy of the homogeneous electron gas; this defines the RPA+ correlation energy $E_{XC}^{RPA+}[n] = E_{XC}^{RPA}[n] + E_C^{sr}[n]$. Note that the RPA+ is exact in the limit of the homogeneous electron gas. Kurth and Perdew[10] showed that E_C^{sr} implies only small corrections to molecular binding energies and suggest that both the RPA and the RPA+ could achieve chemical accuracy for these energies. Alternatively, we include exchange effects, i.e., between like spin electrons, by considering the (approximate) frequency-independent exchange kernel of Petersilka, Gossmann, and Gross[11] (PGG kernel),

$$f_\lambda^{XC-PGG}(\mathbf{r},\mathbf{r}') = -\lambda e^2 \sum_\sigma \frac{\left| \sum_k^{occ} \phi_{k\sigma}^*(\mathbf{r})\phi_{k\sigma}(\mathbf{r}') \right|^2}{n(\mathbf{r})n(\mathbf{r}')|\mathbf{r}-\mathbf{r}'|}. \quad (5)$$

In one- and two-electron systems the PGG exchange kernel is exact: It eliminates unphysical self-correlation and, unlike the RPA or RPA+, leads to zero correlation energy for one electron systems.

So far the above ACFDT formalism has been applied to the (van der Waals) attraction between jellium slabs, as well as the asymptotic atom-atom van der Waals interaction[9,12,13] or, with some simplification, the asymptotic interactions of any neutral fragments.[14] Applications to chemically bonded molecules (and real solids) have been lacking, mainly because solving Eq. (3) for general three-dimensional densities has been considered as computationally intractable. However, recently, Furche has implemented the RPA and RPA+ ACFDT functionals[15] and examined (1) the atomization energies of a dozen of molecules; (2) N_2 equilibrium bond length, vibrational frequency, and dissociation curve. His implementation (based on atomic orbitals) has an overall N^6 scaling, where N is the size of the atomic orbital basis. He finds that the RPA and RPA+ atomization energies are usually smaller than the experimental ones, and have an overall accuracy comparable to the GGA.

In the present work, we analyze the behavior of the three above-defined functionals, for the He atom and the H_2 and Be_2 molecules. We show that the PGG kernel gives a functional qualitatively as accurate as the RPA and the RPA+. In particular, all three are able to describe correctly the bonding of Be_2, a weakly bonded system not examined by Furche, for which LDA and GGA perform poorly. Our implementation, based on plane waves and pseudopotentials, scales as the fourth power of the system size, significantly improving Furche's scaling.
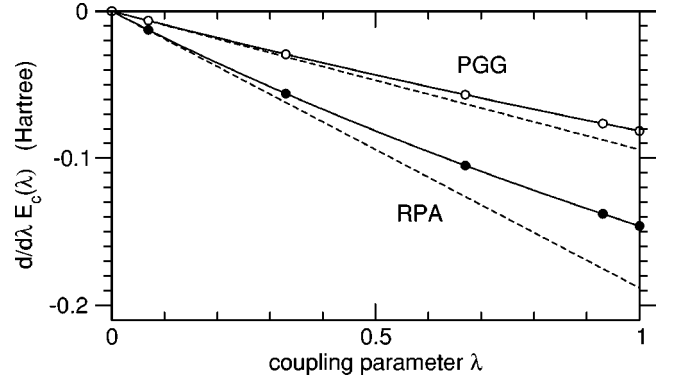

FIG. 1. Full lines: coupling strength decomposition of the correlation energy for the He atom. The area above each curve represents the corresponding correlation energy. Dashed lines: the linear slope of the full lines at $\lambda = 0$.

In our implementation,[16] the system is placed in a large supercell with periodic boundary conditions. The initial Kohn-Sham ground-state calculation is carried out within the LDA. Accurate normconserving nonlocal pseudopotentials are used to represent the electron-ion interactions.[17] The response functions and kernels are treated in the plane-wave representation defined, e.g., for $\chi_{0\mathbf{GG}'}(iu)$, by $\chi_0(\mathbf{r},\mathbf{r}',iu) = \Sigma_{\mathbf{G},\mathbf{G}'}\chi_{0\mathbf{GG}'}(iu)e^{i\mathbf{G}\cdot\mathbf{r}}e^{-i\mathbf{G}'\cdot\mathbf{r}'}$, where $\mathbf{G}$ is a reciprocal-lattice vector. We obtain the Kohn-Sham response function thanks to the sum over states in Eq. (2) and solve the Dyson equation (3) as the system of linear equations

$$\sum_{\mathbf{G}_1,\mathbf{G}_2} (\delta_{\mathbf{GG}_1} - \chi_{0\mathbf{GG}_2}f_{\lambda\mathbf{G}_2\mathbf{G}_1}^{HXC})\chi_{\lambda\mathbf{G}_1\mathbf{G}'} = \chi_{0\mathbf{GG}'}, \quad (6)$$

using the RPA or PGG kernels. To obtain E_{XC} we evaluate the correlation energy as

$$E_C = \int_0^1 d\lambda \frac{\hbar}{2\pi} \int_0^\infty du \sum_\mathbf{G} \frac{4\pi e^2}{G^2}\{\chi_{0\mathbf{GG}}(iu) - \chi_{\lambda\mathbf{GG}}(iu)\}, \quad (7)$$

and add on E_X which we compute similarly.[18] For the λ integration we use the fourth order Gauss-Legendre quadrature which proved to be accurate for the present systems. For the u integration we follow the Gauss quadrature scheme of Ref. 19, using 20 (He), 18 (H_2), and 24 (Be_2) supports, such that the exchange energies calculated from Eqs. (1) and (4) agree to within 1 meV. We solve Eq. (6) repetitively for the particular set of u and λ parameters. Our algorithm scales as $M_{occ}M_{unocc}N^2$ to set up the Kohn-Sham response function and N^3 to solve the Dyson equation, where N is the size of the $\chi_{\lambda\mathbf{GG}'}$ matrices, and M_{occ} (M_{unocc}) is the number of occupied (unoccupied) Kohn-Sham states.

We have carefully tested the convergence of our calculations with respect to the computational parameters involved. For the results reported below we used fcc supercells corresponding to a nearest image distance of 12 (He), 15 (H_2), and 22 bohr (Be_2). The plane-wave cutoff energy in the initial Kohn-Sham calculations was set to 16 (He), 30 (H_2) and 12.5 hartrees (Be_2), and to 12 (He and H_2), and 8 hartrees
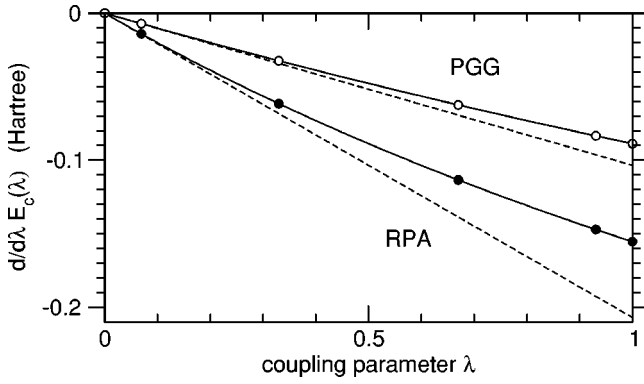
FIG. 2. As in Fig. 1 but for the H_2 dimer with the experimental internuclear distance of 1.4 bohr.

(Be_2) in the calculation of the response functions. The Kohn-Sham response functions included unoccupied states up to eigenenergies of 8 (He), 5.4 (H_2), and 2.5 hartrees (Be_2). Using these parameters we estimate to obtain RPA binding energies to within 30 meV and absolute correlation energies to within 100 meV.

Figures 1 and 2 present the λ integrand of Eq. (7), noted $d/d\lambda\, E_C(\lambda)$, for the two-electron systems He and H_2 (RPA and PGG kernels). Figure 3 shows this quantity for the Be_2 dimer and the two separate Be atoms. The integral of $d/d\lambda\, E_C(\lambda)$ is the correlation energy. Its bending with respect to the linear slope at the origin (displayed in Figs. 1 and 2 by dashed lines) plays an important role in the design of (hybrid) schemes based on the adiabatic-connection formalism[21,22] or Görling-Levy perturbation theory.[23]

From Figs. 1 and 2, it is clear that the RPA and PGG kernels give quite different correlation energies. For the He atom, the RPA E_C is -78 mhartree, while the PGG E_C is -44 mhartree, in excellent agreement with the exact correlation energy[20] of -43 mhartree: the PGG kernel correctly couples only the two opposite spin electrons, while the RPA leads to a spurious self-correlation of the like spin electrons. However, the addition of E_C^{sr} gives the RPA+ value of -43 mhartree, also in excellent agreement with the

TABLE I. Calculated properties of the H_2 dimer. Shown are the binding energy E_b, bond length d_0, and harmonic vibrational frequency ω_e. The zero-point vibrational energy has been subtracted from the experimental value for E_b.

	E_b(eV)	d_0 (bohr)	ω_e (10^3 cm^{-1})
LSDA	-4.92	1.44	4.35
GGA	-4.54	1.41	4.49
EXX	-3.64	1.38	4.63
RPA	-4.72	1.39	4.50
RPA+	-4.75	1.40	4.48
PGG	-4.85	1.40	4.52
Exact [a]	-4.7466	1.4008	
Expt. [b]	-4.75	1.40	4.401

[a]Reference 24.
[b]Cited from Ref. 24.

experiment.[10] For comparison, in the LDA, E_C is -112 mhartree, and in the GGA, E_C is -42 mhartree.

The bending of the curves for He and H_2 shown in Figs. 1 and 2 is rather moderate, but much more pronounced for Be_2, as shown in Fig. 3. The analysis of the latter effect shows that it is due to the small energy separation between the ground-state $(2s)^2$ and the excited $2s2p$ configurations. The correlation energy contribution to the binding energy, shown by the shaded areas, is markedly different when evaluated from the linear slope of the curves at $\lambda=0$, instead from the full curves.

For the H_2 and Be_2 dimers, we have computed the binding energy, bond length, and harmonic vibrational frequencies, and compared them with those obtained in the LDA, GGA, exact Kohn-Sham exchange (EXX), and accurate quantum-chemical treatments, and with respect to experiment. These results are presented in Tables I and II. As concerns binding energies, with both the RPA and RPA+, we reach an excellent 0.04 eV accuracy. As argued by Kurth and Perdew,[10] the RPA error cancels when taking energy differences of systems with the same number of electrons. With the PGG kernel we obtain a slightly lower binding energy
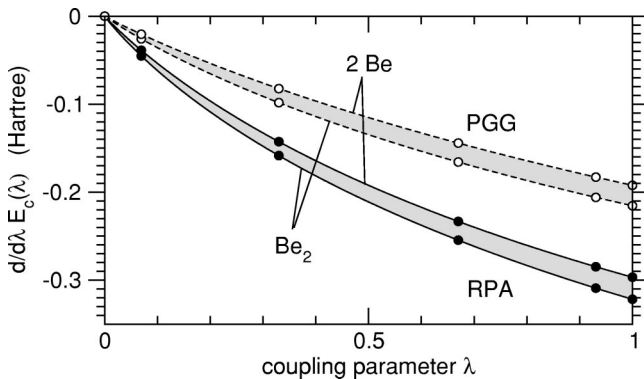

FIG. 3. Coupling strength decomposition of the correlation energy for two Be atoms and the Be_2 dimer with the experimental internuclear distance of 4.63 bohr. The shaded areas give the correlation energy contribution to the binding energy of the Be_2 dimer.

TABLE II. Calculated properties of the Be_2 dimer (see Table I). Values in parentheses have been obtained using a pseudopotential derived from an atomic calculation within the LDA.

	E_b(eV)	d_0 (bohr)	ω_e(cm^{-1})
LSDA	-0.56	4.52	378
GGA	-0.43	4.57	361
EXX	$+0.45(+0.41)$		
RPA	$-0.08(-0.13)$	4.55	311
RPA+	$-0.06(-0.10)$	4.59	298
PGG	$-0.07(-0.12)$	4.60	225
CI [a]	-0.1107	4.627	268.2
Expt. [b]	-0.098	4.63	275.8

[a]Configuration interaction (CI) calculation of Ref. 25.
[b]Cited from Ref. 25.

compared to the RPA in the case of H_2, while for Be_2 it performs as well. Note that Be_2 is a particularly difficult system: bonding and antibonding orbitals are equally occupied, making it a zero bond-order system. Its experimental bonding energy is about 40 times smaller than the one of H_2, and the reasonably successful description of the latter within LDA, GGA, or EXX is at variance with the large overbinding of Be_2 found within LDA or GGA, or the complete lack of binding within EXX. For Be_2, we note that a pseudopotential derived from an atomic calculation within the LDA instead of the EXX resulted in somewhat lower binding energies, as shown in Table. II, without, however, affecting our above conclusions.

As concerns bond lengths and vibrational frequencies for H_2, we obtain reasonable results within RPA, RPA+, and PGG, albeit the associated numerical errors forbid us to claim improvement over LDA and GGA (that are actually quite good). For Be_2, we see some improvement of the bond-length description, and a 60% reduction of the error of the vibrational frequencies compared to experiment. The RPA + and PGG kernel are seen to increase, i.e., improve the bond length compared to the RPA.

The ACFDT density functionals are able to describe van der Waals interactions between separated fragments, as shown by other authors. In the present study, we have implemented three different ACFDT functionals (RPA, RPA+, and PGG) in a plane-wave pseudopotential framework. They deliver accurate molecular properties, even in such a difficult case as Be_2, where LDA, GGA, or EXX fail qualitatively. Although Furche has shown that, for a dozen molecules, the overall error in the binding energies is on the order of the GGA one, we believe that the ACFDT class of functionals has the potential to perform significantly better than the GGA's or hybrid functionals, as the present GGAs have been optimized during several decades. In particular, (1) we have not tried to adjust or to hybridize these functionals, (2) the time-dependent LDA kernel, which defines a fourth functional (see, e.g., Ref. 26), should be implemented, as well as energy-adjusted kernels.[27]

[1] P. Hohenberg and W. Kohn, Phys. Rev. B **136**, B864 (1964).
[2] W. Kohn and L.J. Sham, Phys. Rev. **140**, A1133 (1965).
[3] Several generalized gradient approximations have been proposed. We rely on the one proposed by J.P. Perdew, K. Burke, and M. Ernzerhof, Phys. Rev. Lett. **77**, 3865 (1996), where other GGA's are mentioned.
[4] A.D. Becke, J. Chem. Phys. **98**, 5648 (1993).
[5] K. Burke, M. Ernzerhof, and J.P. Perdew, Chem. Phys. Lett. **265**, 115 (1997).
[6] L.A. Curtiss, K. Raghavachari, P.C. Redfern, and J.A. Pople, J. Chem. Phys. **106**, 1063 (1997).
[7] D.C. Langreth and J.P. Perdew, Solid State Commun. **17**, 1425 (1975); Phys. Rev. B **15**, 2884 (1977).
[8] E. K. U. Gross, J. F. Dobson, and M. Petersilka, in *Density Functional Theory II*, Vol. 181 of *Topics in Current Chemistry*, edited by R. F. Nalewajski (Springer, Berlin, 1996), p. 81.
[9] J.F. Dobson and J. Wang, Phys. Rev. Lett. **82**, 2123 (1999).
[10] S. Kurth and J.P. Perdew, Phys. Rev. B **59**, 10 461 (1999).
[11] M. Petersilka, U.J. Gossmann, and E.K.U. Gross, Phys. Rev. Lett. **76**, 1212 (1996).
[12] M. Lein and E.K.U. Gross, J. Comput. Chem. **20**, 12 (1999).
[13] W. Kohn, Y. Meir, and D.E. Makarov, Phys. Rev. Lett. **80**, 4153 (1998).
[14] E. Hult, H. Rydberg, B.I. Lundqvist, and D.C. Langreth, Phys. Rev. B **59**, 4708 (1999).
[15] F. Furche, Phys. Rev. B **64**, 195120 (2001).
[16] X. Gonze *et al.*, Comput. Mater. Sci. (to be published). Our implementation is part of the ABINIT project, http://www.abinit.org
[17] N. Troullier and J.L. Martins, Phys. Rev. B **43**, 1993 (1991); M. Fuchs and M. Scheffler, Comput. Phys. Commun. **119**, 67 (1999). For the ACFDT functionals, we generate the pseudopotentials from free-atom calculations within exact Kohn-Sham exchange.
[18] In evaluating E_X from Eq. (1) the self-interaction term associated with $n(\mathbf{r})\delta(\mathbf{r}-\mathbf{r}')$ cancels out.
[19] R.W. Godby, M. Schlüter, and L.J. Sham, Phys. Rev. B **37**, 10 159 (1988).
[20] C.J. Umrigar and X. Gonze, Phys. Rev. A **50**, 3827 (1994).
[21] M. Ernzerhof, Chem. Phys. Lett. **263**, 499 (1996).
[22] M. Seidl, J.P. Perdew, and S. Kurth, Phys. Rev. Lett. **84**, 5070 (2000).
[23] A. Görling and M. Levy, Phys. Rev. A **50**, 196 (1994).
[24] W. Kolos and C.C. Roothaan, Rev. Mod. Phys. **32**, 219 (1960).
[25] J. Stärck and W. Meyer, Chem. Phys. Lett. **258**, 421 (1996).
[26] M. Lein, E.K.U. Gross, and J.P. Perdew, Phys. Rev. B **61**, 13 431 (2000).
[27] J.F. Dobson and J. Wang, Phys. Rev. B **62**, 10 038 (2000).